PARTICLE FILTERS FOR RSS-BASED LOCALIZATION IN WIRELESS SENSOR NETWORKS: AN EXPERIMENTAL STUDY

C. Morelli [1], *M. Nicoli* [1], *V. Rampa* [2], *U. Spagnolini* [1], *C. Alippi* [1]
[1] Dip. Elettronica e Informazione, [2] I.E.I.I.T.-C.N.R. Sez. Milano
Politecnico di Milano, Italy; E-mail: {morelli,nicoli,rampa,spagnoli,alippi}@elet.polimi.it

ABSTRACT

This paper focuses on the development of a radio localization technique for a wireless sensor network infrastructure where a large number of simple power-aware nodes are spread in indoor environments. Fixed and moving nodes exchange radio messages but can only measure mutual power figures such as the received signal strength (RSS) indicator. Local maximum likelihood estimation from propagation models suffers from false alarm problems due to incorrect position information, complex indoor propagation effects and simple hardware radio architectures. Here, we propose a Bayesian approach to estimate *and* track the position of a moving node from power maps obtained through field measurements. To lower the computational power required by grid-based algorithms, we exploit particle filter techniques that implement an irregular sampling of the a-posteriori probability space. Finally, experimental results are presented and discussed.

1. INTRODUCTION

Indoor positioning techniques with applications to wireless sensor network (WSN) infrastructures are of great interest nowadays for their wide spectrum applications. A WSN is a very dense network of small, low-powered and low-consuming nodes capable of sensing and storing signals while exchanging messages with other devices. These nodes can sense either electromagnetic fields (i.e., power or signal sensors) or elastic waves (i.e., audio or vibration sensors). Literature about measurement models of both kind is widely available [1], [2]. A great importance is given to the network self-configuration and its ability to dynamically grow up or shrink and accommodate different operational conditions such as unknown node positioning and cell tracking. In fact, a sensor network has a dynamic topology, i.e. anchor nodes (ANs) and moving nodes (MNs) are both present, and nodes can be added or removed. To reduce the communication overhead, WSN positioning schemes work essentially in a proximity context, so that only measurements relative to neighboring nodes are employed. In addition, low-level packet routing strategies must be set up to allow fast, reliable and power-aware communications [2].

In this paper, we are concerned with localization methods based on received signal strength (RSS) measurements, as they are relatively inexpensive and simple to be carried out. We refer to a non-static localization problem, that consists in tracking the position of a MN in an environment with a given layout and with fixed ANs located in known positions. Location estimate can be achieved by exploiting the node infrastructure, i.e. by tracking the most likely subset (*cluster*) of nearest ANs, or by exploiting radio propagation models obtained from field measurements. The first method is rather efficient but inaccurate for most applications while the latter method shows better precision but it is usually very slow. Thus, we propose an experimental localization method that exploits both the network topology *and* a log-normal RSS model [3] integrated with field measurements [4]. Finally, Bayesian filtering [5] is performed in order to alleviate the *false-localization* problem that arises using RSS observations. The MN location sequence is modeled as an hidden Markov model (HMM) and sequentially tracked either by the grid-based Detection/Tracking Algorithm (D/TA, [5]) or through a canonical Sequential Importance Resampling (SIR) particle filtering (PF) [6]. The algorithms are centralized, but a distributed scheme is possible as shown in [7]. The tracked MN position is also used to predict the next cluster of nearest nodes. Simulations performed on experimental measurements show that high accuracy localization is obtained by the proposed approach.

The paper is organized as follows: the localization problem is presented in Sec. 2, where measurement and network models are proposed. Sec. 3 introduces the HMM framework and the tracking algorithms, whose performances are studied in Sec. 4 using measures from a real field campaign. Sec. 5 draws some conclusions.

2. PROBLEM FORMULATION

We consider a WSN spread in an indoor planar region $\mathcal{X} \subset \mathbb{R}^2$. A node is moving within $\mathcal{X}$ while all the others are fixed. We also assume that L ANs are placed in known positions $\mathbf{z}^{(\ell)} = [z_1^{(\ell)}, z_2^{(\ell)}] \in \mathcal{X}$, where $z_i^{(\ell)}$ denotes the ith Cartesian coordinate in the two-dimensional (2D) space ($i = 1, 2$; $\ell = 1, \ldots, L$). These known positions can be either measured during the deployment or estimated by the WSN itself by using a cooperative localization algorithm [2],[7].

This paper is concerned with the problem of real-time localization. At any discrete time instant $t \in \mathbb{N}$, the MN position $\mathbf{x}_t = [x_{1,t}, x_{2,t}] \in \mathcal{X}$ is not directly observable but it is hidden into L measurements $\mathbf{y}_t = [y_{1,t}, \ldots, y_{L,t}]^{\mathrm{T}}$ exchanged between the MN and the L ANs. Each observation $y_{\ell,t}$ represents the power of the signal received, expressed in dBm, over the ℓth AN-MN link.

If these RSS measurements could be reliably described by a statistical model, then it would be possible to derive the estimate $\hat{\mathbf{x}}_t$ of the MN position through conventional estimation methods. This is the rationale for the local maximum likelihood estimation (MLE) approach applied to the current measurement $\mathbf{y}_t$. Likewise, based on the Markovian state-space model, a Bayesian approach could be to used to estimate the unobserved motion $\mathbf{x}_{1:t}$. In this case, all measurements $\mathbf{y}_{1:t}$ up to the current time instant are exploited by a tracking algorithm that refines the a-posteriori probabilities of the states. The definition of a precise RSS model is crucial for the accuracy of these localization methods.

2.1. RSS model

Analytical models are usually adopted to describe the relationship between the measured power $y_{\ell,t}$ and the MN position. Yet, localization methods based on such models are mostly inaccurate, as the

This work has been funded by the Virtual Immersive Communications (FIRB-VICom) Project of the Italian Ministry of Education, University and Research.

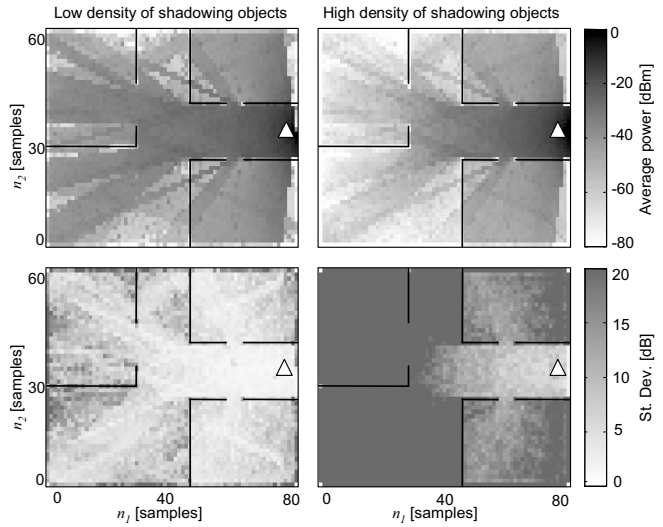

Fig. 1. Raytracing simulation of RSS average (top) and fluctuations (bottom) for a given AN (triangle). The propagation accounts for N shadowing objects randomly moving within the area, each simulating a person as a cylinder of radius $r = 20$cm: $N = 5$ (left) or $N = 40$ (right). For increasing object density, the RSS average is almost invariant, while the variance increases.

received power is strongly affected by unpredictable multipath and shadowing effects that depend on the specific indoor environment (i.e., the physical arrangement of objects in the room) and errors due to the simple radio devices employed in WSN nodes. In order to guarantee robustness against mismodeling, in this paper we propose a different approach: we define a log-normal statistical model whose parameters are tailored to the specific indoor environment by exploiting experimental measurements gathered during an off-line calibration phase.

Each RSS measurement $y_{\ell,t}$ [dBm] is expressed by:

$$y_{\ell,t} = \bar{y}_\ell(\mathbf{x}_t) + v_{\ell,t}. \quad (1)$$

The first deterministic term $\bar{y}_{\ell,t}(\mathbf{x}_t)$ [dBm] indicates the attenuation due to propagation and to static obstructions (e.g., walls and furniture), while the additive Gaussian random noise $v_{\ell,t} \sim \mathcal{N}(0, \sigma^2_\ell(\mathbf{x}_t))$, with zero mean and standard deviation $\sigma_\ell(\mathbf{x}_t)$ [dB], accounts for the randomness of shadowing (e.g., due to objects or people moving over the environment). Such a model was validated by raytracing simulations [8] for a typical indoor environment, as shown in Fig. 1. These numerical results confirm that not only the expected value but also the standard deviation of (1) depends on the position $\mathbf{x}_t$. Notice that time-varying measurement errors due to additive noise or interference are not considered, as we assume that multiple observations can be averaged over time to reduce the impact of such errors.

As far as localization is concerned, we assume complete knowledge of the power mean $\bar{y}_\ell(\mathbf{x})$ and the shadowing standard deviation $\sigma_\ell(\mathbf{x})$ for all positions $\mathbf{x} \in \mathcal{X}$ and all ANs, as these values are measured during the preliminary off-line calibration phase. Practically, our experimental localization approach is carried out in two steps:
1. Off-line calibration: a node is subsequently placed in M different positions $\{\mathbf{z}_m\}_{m=1}^M \in \mathcal{X}$; at each position and for each AN, time samples are read from the RSS indicator and they are used to evaluate a sample average $\bar{y}_\ell(\mathbf{z}_m)$ and a sample standard deviation

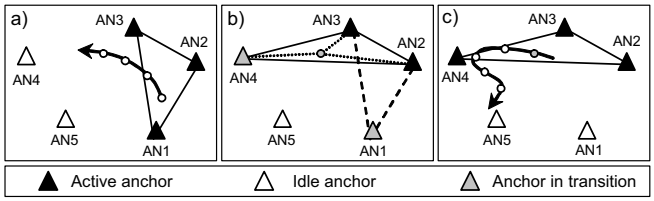

Fig. 2. Cluster tracking: a) four subsequent positions estimated within a cluster; b) transition to the new cluster; c) four subsequent positions estimated within the updated cluster.

$\sigma_\ell(\mathbf{z}_m)$. Interpolation [9] is then performed to derive 2D maps of the RSS mean and standard deviation for the whole space $\mathcal{X}$.
2. On-line tracking: at each time instant t, each AN measures the RSS of the signal received from the MN. All these L RSS measurements, together with the statistical maps and the knowledge of the WSN topology, are used by the localization algorithms to estimate the MN position.

2.2. Clustering of ANs: cluster tracking

In a dense network of low-powered sensors, it is convenient to estimate the MN location using only the RSS measurements gathered by a cluster of $\tilde{L} < L$ ANs in the proximity of the MN. This allows to save sensor energy and to improve the localization accuracy by neglecting noisy RSS measurements recorded by distant APs. This approach is illustrated in Fig. 2: it consists in tracking both the MN within the active cluster and the cluster itself using two different time scales. The MN estimate is updated every time instant, while the AN cluster composition is computed every $N_t \geq 1$ time instants depending on the MN velocity. At time instant $t = 1, N_t + 1, 2N_t + 1, ...$ the cluster is rebuilt by activating only the subset of $\tilde{L}$ nodes that are closest to the last position estimate $\hat{\mathbf{x}}_{t-1}$, while the other $L - \tilde{L}$ nodes are put on hold. During the initialization phase ($t = 1$), if no a-priori information is available about the MN position, all the L ANs are used for the first localization and then a starting cluster is selected according the estimate $\hat{\mathbf{x}}_1$. The best results are obtained for $N_t = 1$, but higher values reduce the computational complexity.

3. MN TRACKING ALGORITHMS

In this section, we introduce the Bayesian framework used for the on-line sequential estimation of the MN position. At first, a non-linear and non-Gaussian HMM is defined, then two algorithms are proposed for the state-sequence estimation: the grid-based approach D/TA (developed for ultra-wide band radar systems [5]) and the PF method (also known as sequential Monte Carlo) [6].

3.1. HMM and grid-based filtering

The MN location sequence $\mathbf{x}_{1:T}$ is modeled as an homogeneous first-order Markov process, described by the system equation $\mathbf{x}_t = \mathbf{x}_{t-1} + \mathbf{v}_t$, where $\mathbf{v}_t$ denotes the driving process. The probabilistic model of the state evolution is defined according to the known distribution $f_\mathbf{v}(\mathbf{v})$ of the driving process: $p(\mathbf{x}_t|\mathbf{x}_{t-1}) = f_\mathbf{v}(\mathbf{x}_t - \mathbf{x}_{t-1})$. The initial state distribution $p(\mathbf{x}_1)$, for any $\mathbf{x}_1 \in \mathcal{X}$, is chosen based on the available a-priori information about the MN position at time $t = 1$: it can be either uniform in case of missing a-priori information or impulsive in case of knowledge of the starting location [5].

The state $\mathbf{x}_t \in \mathcal{X}$ is hidden into the observation $\mathbf{y}_t \in \mathbb{R}^L$, while, as usual, the observations $\{\mathbf{y}_t\}$ are assumed to be conditionally inde-

pendent given the process $\mathbf{x}_t$. Recalling the model (1) and assuming independence between the AN observations, the $L \times 1$ measurement vector $\mathbf{y}_t$, conditioned to state $\mathbf{x}_t$, is an uncorrelated Gaussian vector with mean $\bar{\mathbf{y}}(\mathbf{x}_t) = [\bar{y}_1(\mathbf{x}_t) \cdots \bar{y}_L(\mathbf{x}_t)]^{\mathrm{T}}$ and covariance matrix $\mathbf{C}(\mathbf{x}_t) = \mathrm{diag}(\sigma_1^2(\mathbf{x}_t), \ldots, \sigma_L^2(\mathbf{x}_t))$. Thus, the conditioned distribution is:

$$p(\mathbf{y}_t|\mathbf{x}_t) = \frac{1}{(2\pi)^{L/2}|\mathbf{C}(\mathbf{x}_t)|^{1/2}} \exp\left\{-\frac{1}{2}\left\|\mathbf{y}_t - \bar{\mathbf{y}}(\mathbf{x}_t)\right\|^2_{\mathbf{C}^{-1}(\mathbf{x}_t)}\right\} \tag{2}$$

where $\|\mathbf{y}\|^2_{\mathbf{C}} = \mathbf{y}^{\mathrm{H}}\mathbf{C}\,\mathbf{y}$ is the square norm of the vector $\mathbf{y}$ weighted by the matrix $\mathbf{C}$. For the idle ANs (those out of the active cluster), we set $y_{\ell,t} = \bar{y}_\ell(\mathbf{x}_t) = 0$ and $\sigma^2_\ell(\mathbf{x}_t) = \mathrm{const}$ for all $\mathbf{x}_t \in \mathcal{X}$, in order to null their contribution to the conditioned probability.

A local estimate of the state $\mathbf{x}_t$ can be obtained by applying the MLE criterion only: $\hat{\mathbf{x}}_t = \arg\max_{\mathbf{x}_t \in \mathcal{X}} p(\mathbf{y}_t|\mathbf{x}_t)$. Yet, we are interested in a Bayesian approach that exploits the previously defined dynamic model to evaluate the a-posteriori probability density function (pdf) $p(\mathbf{x}_t|\mathbf{y}_{1:t})$ given the whole measurement set $\mathbf{y}_{1:t}$. The a-posteriori pdf depends on the (memory-less) likelihood function $p(\mathbf{y}_t|\mathbf{x}_t)$ and the a-priori (memory-bearing) pdf $p(\mathbf{x}_t|\mathbf{y}_{1:t-1})$, according to:

$$p(\mathbf{x}_t|\mathbf{y}_{1:t}) \propto p(\mathbf{y}_t|\mathbf{x}_t)p(\mathbf{x}_t|\mathbf{y}_{1:t-1}), \tag{3}$$

where constant terms have been neglected. The a-priori conditional distribution function is be obtained as:

$$p(\mathbf{x}_t|\mathbf{y}_{1:t-1}) = \int_{\mathcal{X}} p(\mathbf{x}_t|\mathbf{x}_{t-1})p(\mathbf{x}_{t-1}|\mathbf{y}_{1:t-1})d\mathbf{x}_{t-1} \tag{4}$$

for any $t > 1$, while it is initialized with $p(\mathbf{x}_t|\mathbf{y}_{1:t-1}) = p(\mathbf{x}_1)$ for $t = 1$. Once the a-posteriori pdf is calculated from (3), the estimate of the state $\mathbf{x}_t$ can be obtained using either the maximum-a-posteriori (MAP) or minimum mean square error (MMSE) criterion.

In particular, the grid-based D/TA approach [5] relies on a uniform 2D sampling of the continuous state space $\mathcal{X}$. The MN location $\mathbf{x}_t$ is assumed to take values within a regular grid $\mathcal{X}_N$ composed of $N = N_1N_2$ spatial positions, $\mathbf{n}\Delta x = [n_1, n_2]\Delta x$, with sampling interval Δx, $n_1 = 1, \ldots, N_1$ and $n_2 = 1, \ldots, N_2$. Equation (4) is thus approximated by a finite sum. The MN position MAP estimate is obtained by a forward-only HMM-based tracking algorithm that calculates (3) and then computes: $\hat{\mathbf{x}}_t = \arg\max_{\mathbf{x}_t \in \mathcal{X}_N} p(\mathbf{x}_t|\mathbf{y}_{1:t})$. The disadvantage of such an approach is that the uniform grid must be dense enough to get high localization resolution, thus leading to a large computational load for the evaluation of (3). Still, efficient implementations might be derived keeping into account the locality of the random walk model and by introducing a reduced tracking gate.

3.2. Particle filtering (PF)

The PF approach approximates the a-priori pdf $p(\mathbf{x}_t|\mathbf{y}_{1:t-1})$ with a sum of K Dirac pulses equally weighted and centered on a subset $\{\mathbf{x}_t^{(k)}\}_{k=1}^K \in \mathcal{X}$ of *particles* [6]. This subset is finite and discrete but not uniformly sampled as the regular grid used in the D/TA case. Each particle is sampled from a random variable $\mathbf{x}_t$ with pdf $p(\mathbf{x}_t|\mathbf{y}_{1:t-1})$. In the following part of the paper, this will be indicated briefly as: $\mathbf{x}_t^{(k)} \sim p(\mathbf{x}_t|\mathbf{y}_{1:t-1})$. For large K, we assume that following approximation holds true:

$$p(\mathbf{x}_t|\mathbf{y}_{1:t-1}) \approx \frac{1}{K}\sum_{k=1}^{K} \delta(\mathbf{x}_t - \mathbf{x}_t^{(k)}). \tag{5}$$

A-posteriori pdf becomes $p(\mathbf{x}_t|\mathbf{y}_{1:t}) \approx \sum_k w_t^{(k)}\delta(\mathbf{x}_t - \mathbf{x}_t^{(k)})$, where each *weight* $w_t^{(k)}$ is proportional to $p(\mathbf{y}_t|\mathbf{x}_t^{(k)})$ and it is normalized so that $\sum_k w_t^{(k)} = 1$. Thus, the a-posteriori pdf is completely identified by the tuples $\{\mathbf{x}_t^{(k)}, w_t^{(k)}\}_{k=1}^K$. The MMSE estimate of the state $\mathbf{x}_t$ at instant t is the expectation $\hat{\mathbf{x}}_k = \mathrm{E}[\mathbf{x}_t]$ which is computed as the weighted mean $\hat{\mathbf{x}}_k \approx \sum_{k=1}^K w_t^{(k)}\mathbf{x}_t^{(k)}$.

Given the tuples $\{\mathbf{x}_t^{(k)}, w_t^{(k)}\}_{k=1}^K$, the new particles $\{\mathbf{x}_{t+1}^{(k)}\}_{k=1}^K$ at time $t+1$ can be generated according the following steps: *i*) by executing a resampling process of the current particles according to their weights and *ii*) by making them evolve through the state equation. This is known as the SIR variant of a PF. In the first step (i.e., the *resampling* step), the particles $\{\mathbf{x}_t^{(m)}\}_{m=1}^K$ are resampled in a new set $\{\tilde{\mathbf{x}}_t^{(k)}\}_{k=1}^K$ such that $\forall k\ P(\tilde{\mathbf{x}}_t^{(k)} = \mathbf{x}_t^{(m)}) = w_t^{(m)}$; this can be done both in a deterministic way or randomly [6]. According to this method, particles with negligible weights are dropped while particles with strong weights are dismantled in a lot of smaller and uniform particles with $\tilde{w}_t^{(k)} = \frac{1}{K}$. The second step (i.e., the *forwarding* step) consists in sampling transitions $\mathbf{v}_{t+1}^{(k)} \sim f_{\mathbf{v}}(\mathbf{z})$ and in evaluating $\mathbf{x}_{t+1}^{(k)} = \tilde{\mathbf{x}}_t^{(k)} + \mathbf{v}_{t+1}^{(k)}$ for each resampled particle, so that the new set of a-priori particles $\{\mathbf{x}_{t+1}^{(k)}\}_{k=1}^K$ is obtained. At the first iteration ($t = 1$) the a-priori particle distribution is initialized as $\mathbf{x}_1^{(k)} \sim p(\mathbf{x}_1)\ \forall k$. Improved PF or optimized choices of the importance function may be employed to improve the algorithm effectiveness [6],[10].

4. VALIDATION ON EXPERIMENTAL DATA

Performances of the proposed localization methods have been evaluated by an experimental study carried out with MICA2 Motes at the Politecnico di Milano [4]. As shown in Fig. 3, the WSN was composed of $L = 6$ ANs (indicated as triangles) spread in an indoor environment having size 10.2m×7.5m. During the calibration step, a MN was placed at $M = 92$ different locations. For each position, RSS measurements were collected by the ANs for a time interval of 2 minutes (i.e., 1 value per second) and sent to a Personal Computer for further processing by means of a pivot node. After calibration, RSS measurements were interpolated [9] to produce 2D maps of power mean and standard deviation, sampled at spatial interval $\Delta x = 0.1$m.

The MN path $\mathbf{x}_{1:T}$ was simulated off-line, for a total length of $T = 60000$ locations, according a first-order Markov process with conic-shaped distribution $f_{\mathbf{v}}(\mathbf{v})$ of radius $\epsilon = 0.4$m (see [5] for details). The RSS measurements $\mathbf{y}_{1:T}$ exchanged between the MN and the ANs were simulated by sequentially accessing the experimental database built during the calibration phase. Then, we applied the local MLE, the D/TA, and the PF methods to the measurements $\mathbf{y}_{1:T}$, in order to estimate the MN trajectory. The cluster used for localization was composed of $\tilde{L} = 3$ ANs, and it was tracked using a time step of $N_t = 5$ samples.

Localization performances are shown in Fig. 3 in terms of root mean square error (RMSE) of the estimate as a function of the MN position over the $N_1 \times N_2$ grid $\mathcal{X}_N$. If $\mathcal{I}(\mathbf{x})$ denotes the set of time instants in which the MN trajectory flows across $\mathcal{X}_N$, the RMSE is computed as: $\mathrm{RMSE}(\mathbf{x}) = \{|\mathcal{I}(\mathbf{x})|^{-1}\sum_{t\in\mathcal{I}(\mathbf{x})}(\mathbf{x} - \hat{\mathbf{x}}_t)^2\}^{1/2}$ where $|\cdot|$ denotes the set cardinality. Notice that, unlike MLE and D/TA, the PF estimates do not belong to the regular grid of states.

Examples of tracked trajectory are shown in Fig. 3-a1-a2-a3, for a path $T = 100$ steps long, here forced to be smooth only for visualization purposes. Estimate errors are indicated as lines connecting the true and the estimated positions. Fig. 3-b1-b2-b3 show the RMSE maps for MLE, D/TA and PF, respectively. A detail is shown in Fig. 3-c1-c2, where the RMSE performances are plotted along the 1D sections taken at $n_2 = 2$m (Fig. 3-c1) and $n_1 = 2.5$m

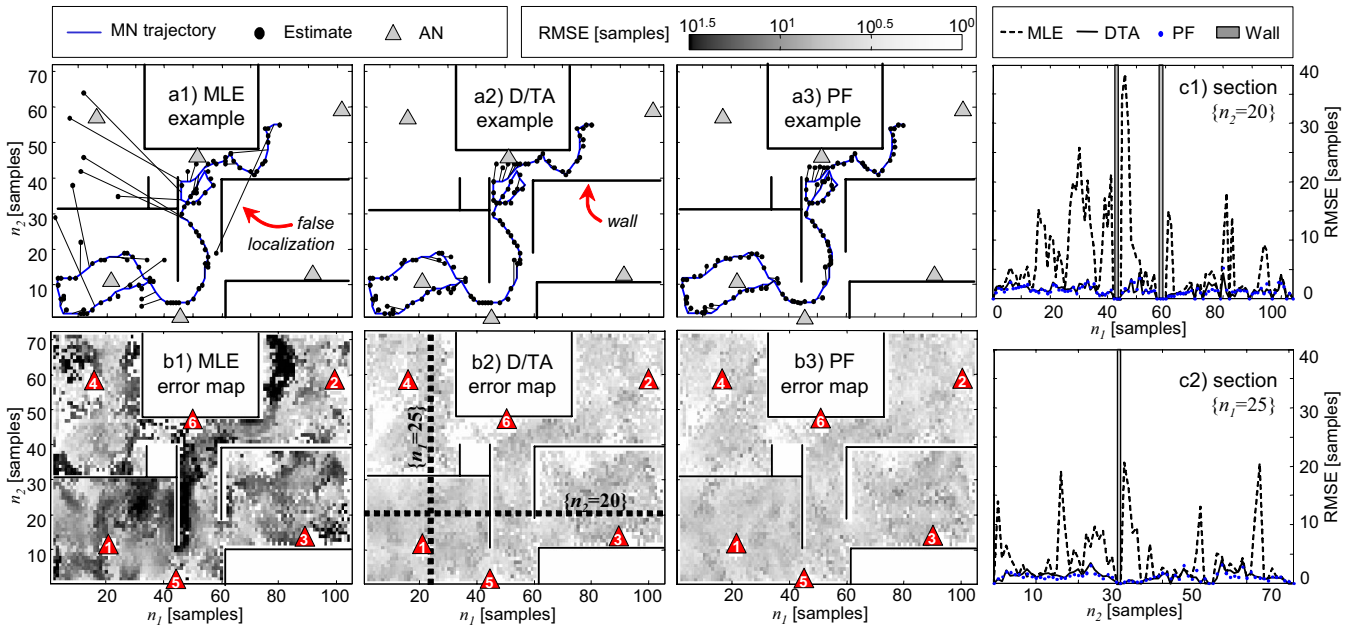

Fig. 3. Estimate performances: a) examples of MN trajectory and relative estimation with MLE (a1), D/TA (a2) and SIR PF (a3); b) Computation of RMSE as a function of MN position for MLE (b1), D/TA (b2) and SIR PF methods (b3); c) slices from RMSE maps, according to section pointed in Fig. b2. Spatial sampling is $\Delta x = 0.1$ m.

(Fig. 3-c2), respectively. MLE performance in Fig. 3-a1-b1 is affected by false-localization problems all over the layout (errors up to 5m). In the same conditions, the Bayesian filters (Fig. 3-a2-a3-b2-b3) reduce the error below 0.5m.

5. CONCLUSIONS

A technique for localization of moving nodes in WSNs has been presented. The proposed algorithm combines a log-normal RSS model with power maps, obtained from experimental field data, to estimate and track the MN position and the cluster of neighboring ANs. Efficient tracking is performed using the PF approach. Experimental results show that the computational complexity can be reduced still achieving high accuracy in the estimation of the position.

6. ACKNOWLEDGMENTS

The authors would like to thank A. Bosisio and M. Spera for validating the RSS model and for simulation results in Fig. 1, and A. Galbiati for the software for spatial interpolation of the power maps.

7. REFERENCES

[1] D. Li, K. D. Wong, Y. H. Hu, A. M. Sayeed, "Detection, classification and tracking of targets," *IEEE Signal Processing Magazine*, Vol. 19, No. 2, pp. 17-29, Mar. 2002.

[2] N. Patwari, J.N. Ash, S. Kyperountas, A.O. Hero, R.L. Moses, N.S. Correal, "Locating the nodes: cooperative localization in wireless sensor networks," *IEEE Signal Processing Magazine*, Vol. 22, No. 4, pp. 54-69, July 2005.

[3] B. L. Mark and Z. R. Zaidi, "Robust mobility tracking for cellular networks," *IEEE Proc. ICC '02*, vol. 1, pp. 445-449, May 2002.

[4] C. Alippi and G. Vanini, "Wireless sensor networks and radio localization: a metrological analysis of the MICA2 received signal strength indicator," *IEEE Proc. LCN '04*, pp. 579-580, Nov. 2004.

[5] C. Morelli, M. Nicoli, V. Rampa, U. Spagnolini, "Hidden Markov Models for radio localization of moving terminals in LOS/NLOS conditions," *IEEE Proc. ICASSP '05*, Vol. 4, pp. 877-880, Mar. 2005.

[6] M. S. Arulampalam, S. Maskell, N. Gordon , T. Clapp, "A tutorial on particle filters for online nonlinear/non-Gaussian Bayesian tracking," *IEEE Trans. Signal Processing*, Vol. 50, No. 2, pp. 174-188, Feb. 2002.

[7] M. Coates, "Distributed particle filters for sensor networks," *ACM Proc. IPSN '04*, pp. 99-107, Apr. 2004.

[8] A.V. Bosisio, U. Spagnolini, "Indoor localization by attenuation maps: model-based interpolation for random medium," *Proc. ICEAA '05*, pp. 1-4, Sept. 2005.

[9] G. Bolondi, F. Rocca, S. Zanoletti, "Automatic contouring of faulted subsurfaces," *Geophysics*, Vol. 41(6), pp. 1379-1393, 1976.

[10] M.K. Pitt and N. Shephard, "Filtering via Simulation: Auxiliary Particle Filters," *Journal of the American Statistical Association*, Vol. 94 (446), pp. 590-599, 1999.